Advective heat transport modelling in aquifers

Ron Coutts
Ardent Innovation Inc., Calgary, Alberta, Canada

ABSTRACT
Recently there has been increasing need for quantitative analysis of advective heat transport in aquifers for projects such as in-situ thermal bitumen recovery and geothermal energy system design. This paper presents the fundamentals of an advective heat transport analysis including estimation of heat transport velocity from aquifer heat capacity values and Darcy velocity. A coupled groundwater and heat transfer numerical model is verified and used to illustrate the effect and importance of accounting for temperature dependent water viscosity when undertaking an advective heat transport analysis. Simulation of thermal plume evolution through time in the case of an aquifer intersected by a hot thermal well illustrates the necessity of three-dimensional (3D) modelling in specific cases.

RÉSUMÉ
Récemment, il y a une demande pour des analyses quantitatives de transfert de chaleur avec advection dans les nappes phréatiques dans le cadre de projets tels que la récuperation in situ de bitume par chauffage et la conception de systèmes géothermiques. Cet article présente les équations de transfert thermique avec advection ainsi que celle permettant d'estimer la vitesse du transfert en fonction de la capacité thermique de l'aquifer et de la vitesse de Darcy. Un modèle numérique couplé de transfert de masse et de chaleur a été vérifié et utilisé pour illustrer l'importance de la viscosité de l'eau dans ce type d'analyse. La simulation de l'évolution de panache thermique pour un aquifer avec des puits thermiques chauds démontre bien la nécessité d'une modélisation 3D dans certains cas.

1 INTRODUCTION

Quantitative analysis of advective-conductive heat transport is increasingly required for a variety of projects including geothermal energy systems and in-situ thermal bitumen recovery.

Thermal wells are used in geothermal energy applications to transfer heat energy between surface facilities and the subsurface. In these applications the ground around the thermal well acts as an energy repository where heat energy is seasonally extracted or stored. Depending on the energy design of the geothermal energy system, groundwater flow in the vicinity of the geothermal well, or wells, may help or hinder the functioning of the system. This may be especially true for larger geothermal energy installations utilizing multiple thermal wells. In these cases, excess or deficit heat plumes transported by groundwater may negatively impact down-gradient thermal wells resulting in underperformance of the overall geothermal energy system.

In Alberta, vast bitumen reserves are located in sand deposits, 90% of which are too deep for open pit mining. To access this resource, in-situ thermal techniques such as cyclic steam stimulation (CSS) and steam assisted gravity drainage (SAGD) are used to extract the bitumen. Both of these technologies utilize thermal wells that are heated in excess of 200 °C and which intersect quaternary aquifers. The heat may cause geochemical changes such as elevated dissolved constituent concentrations by dissolution of soil minerals. Although the exact geochemical changes that may occur when aquifer groundwater is heated and cooled are still being investigated, it is nonetheless important to determine the time evolution of the heat transport from these thermal wells.

In practice the terms "advection" and "convection" can lead to confusion. The term "advection" is used by hydrogeologists to refer to the component of mass or heat transport that occurs by the bulk motion of flowing groundwater. Mechanical engineers dealing with heat transfer in porous media refer to this same process as "forced convection", which is distinct from "passive convection". The latter occurs when fluid flow is established by fluid density variations within a system, typically caused by a heterogeneous temperature distribution. Herein, the terms "advection" and "convection" (short for "forced convection") may be used synonymously.

This paper presents the concept of heat transport velocity, which is useful for quickly calculating the expected heat transport distance along a groundwater flow path. To understand how the heat transfer velocity is derived, the governing equations for groundwater flow and convective-conductive heat transport are presented first as background information.

A finite element model based on the aforementioned governing equations was created and used to compute advective heat transport. Verification of the numerically computed results is demonstrated by comparison with an analytic solution and by comparison with the thermal plume transport distance based on the heat transport velocity.

The numerical model was used to assess the effect of temperature dependent water viscosity on advective heat transport. The model was also used to demonstrate the necessity of considering all three spatial dimensions when computing advective heat transport in specific cases such as a thin confined aquifer intersected by a vertical thermal well.

2 HEAT TRANSPORT VELOCITY

When dealing with advective heat transport situations, it is quite beneficial to have some estimate of the expected travel velocity of the thermal plume. This can be used in the field when deciding on locations of monitoring wells, or in simple cases to verify that a numerical model of advective heat transport is computing correct results.

The derivation of the heat transport velocity comes from consideration of the governing equations for groundwater flow and convective-conductive heat transfer as outlined in the following sections. The governing equations presented here were also solved using a finite element model as discussed later.

2.1 Steady-State Groundwater Flow Equation

Steady-state groundwater flow is governed by the following partial differential equation (PDE):

$$div(-K_H \cdot grad(H)) = 0 \qquad [1]$$

Where:
H = groundwater head (m)
K_H = isotropic saturated hydraulic conductivity (m/d)
grad() = gradient operator
div() = divergence operator

Units shown for the variables in the equations are typical units used in the work presented herein; however, generally any consistent system of mass, length and time units could be used.

In Equation 1, the gradient and divergence operators can be expanded as:

$$grad(H) = \frac{\partial H}{\partial x_i} \qquad [2]$$

$$div(q_H) = \frac{\partial \vec{q}}{\partial x_i} \qquad [3]$$

$$\vec{q}_H = -K_H \cdot grad(H) \qquad [4]$$

Where:
x = a spatial dimension
i = 1, 2 or 3 subscripts refer to spatial dimension
$\vec{q}_H$ = hydraulic flux (Darcy velocity) vector

The PDE for steady-state groundwater flow (Equation 1) essentially states that groundwater flow into an elemental volume of the porous medium equals the flow out of the storage medium at any point in time.

It should be noted that the hydraulic conductivity is a function of the permeability of the porous medium and the water viscosity. Therefore the hydraulic conductivity in Equation 1 is a function of groundwater temperature because water viscosity is temperature dependent.

2.2 Convective-Conductive Heat Transport Equation

The following PDE describes transient convective-conductive heat transport in a saturated porous medium (Neild and Bejan, 2006):

$$div(K_T \cdot grad(T)) - C_W \cdot \vec{q}_H \cdot grad(T) + Q_T = C_M \frac{\partial T}{\partial t} \qquad [5]$$

Where:
T = temperature (°C)
K_T = thermal conductivity (kJ/m-d-°C)
C_W = heat capacity of water (kJ/m^3-°C)
C_M = heat capacity of porous medium (water and soil grain solids combined) (kJ/m^3-°C)
Q_T = heat flux source/sink (kJ/m^3-d)
t = time (days)

The first and second terms on the left-hand-side of Equation 5 represent conductive (diffusive) and convective (advective) heat transport, respectively. The term on the right-hand-side represents the change in storage of heat within an elemental volume of porous medium over time. Note that if the Darcy velocity were zero, then there would be no convective heat transport and Equation 5 would describe only conductive heat transport through time.

The heat capacity of a saturated porous medium is computed as the volumetric weighted average of the heat capacities of the soil grains and the water:

$$C_M = (1-n) \cdot C_S + n \cdot C_W \qquad [6]$$

Where:
C_S = heat capacity of soil grains (kJ/m^3-°C)
n = porosity

Note that Equations 1 and 5 are coupled via the Darcy velocity and therefore must be solved simultaneously.

3.1 Groundwater and Heat Transport Velocities

The Darcy velocity (Equation 4) represents the hydraulic flux of water across a unit area of porous medium. The average linear groundwater flow velocity is distinct from the Darcy velocity in that it represents the advective transport rate of an inert chemical (conservative tracer) introduced into the groundwater flow field. A conservative tracer does not chemically react or absorb/desorb on soil grains. The average linear velocity is higher than the Darcy velocity because part of the cross-sectional flow area perpendicular to the flow direction is occupied by solid soil grains. The average linear velocity is defined as:

$$\vec{v}_H = \frac{\vec{q}_H}{n} \qquad [7]$$

The average linear velocity serves as an upper bound of the heat transport velocity since advective heat transport is analogous to chemical diffusive-advective transport in porous media. Heat cannot transport advectively faster than the groundwater flows through the soil. If the soil grain solids had zero heat capacity, (which is not physically possible), then heat transport would transport exactly like a conservative tracer. Since the soil grains have a non-zero heat capacity, it is clear that the heat transport velocity must be less than the average linear flow velocity. It is also clear that the heat transport velocity depends on the porosity as well.

To determine the expected heat transport velocity, it is necessary to again consider the governing PDE that describes convective-conductive heat transport. Equation 8 below is identical to Equation 5 presented earlier except that the heat source/sink term is zero and all terms have been divided by the heat capacity of the porous medium, C_M.

$$div\left(\frac{K_T}{C_M}\cdot grad(T)\right) - \frac{C_W}{C_M}\cdot \vec{q}_H \cdot grad(T) = \frac{\partial T}{\partial t} \qquad [8]$$

When the PDE is expressed in this way it can be seen that the heat (thermal) transport velocity is given by:

$$\vec{v}_T = \left(\frac{C_W}{C_M}\right)\cdot \vec{q}_H = \left(\frac{C_W}{(1-n)\cdot C_S + n\cdot C_W}\right)\cdot \vec{q}_H \qquad [9]$$

Instructively, note that in Equation 9 when porosity is set to one, (physically impossible), the heat transport velocity equals the Darcy velocity. Furthermore, if the heat capacity of the soil grains is set to zero, (also physically impossible), then the heat transport velocity would equal the average linear velocity.

Knowing that the heat capacity of water varies relatively little as a function of temperature, and knowing that the heat capacity of soil grains also varies relatively little as a function of the typical mineralogy of porous media, it is possible to roughly estimate the ratio of the heat capacities (or heat transport factor) in Equation 9.

Using the relevant soil and water properties in Table 1, the heat transport velocity was computed using Equation 9 as a function of porosity. Figure 1 compares the calculated heat transport velocity as a function of porosity. Average linear velocity is also shown for comparison. Note that the Darcy velocity in Figure 1 is normalized to a unit velocity.

At a typical porosity of 25% and using the heat capacity values stated earlier, the heat transport velocity is 1.60 times the Darcy velocity. Furthermore, the heat transport velocity has only slight variation over the range of porosity values for typical soils as is evident in Figure 1. For example, the relative heat transport velocity for porosities of 15% and 40% are 1.74 and 1.43, respectively. Therefore for practical purposes, heat transport velocity can be roughly estimated as 1.6 times the Darcy velocity for a wide variety of soils in the absence of more detailed information.

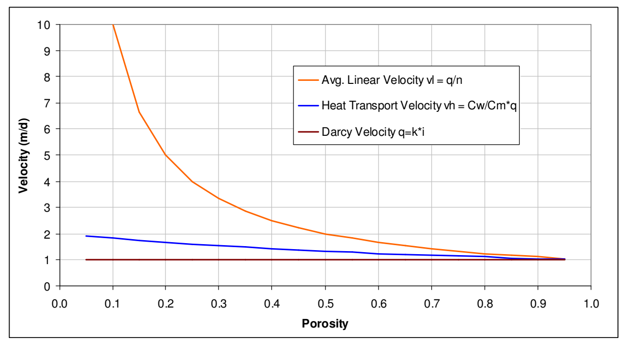

Figure 1. Comparison of Groundwater Velocities as a Function of Porosity

3 NUMERICAL MODEL VERIFICATION

The coupled PDEs for steady-state groundwater flow (Equation 1) and convective-conductive heat transport (Equation 5) were solved using a finite element program. The numerical results were verified as correct by comparing them against an analytic solution in one case and in another case by comparison to the hand-calculated heat transport distance based on heat transport velocity from Equation 9.

3.1 Comparison to an Analytic Solution

An analytic solution for convective-conductive heat transfer available in Hoffman, 2001, was used to verify correct setup and computational capability of the finite element model. The analytic solution is for a one-dimensional fluid flow case where fluid is instantaneously forced through a porous media layer of 1 cm thickness at a Darcy velocity of 25 cm/s. The thermal diffusivity of the layer was 0.01 cm^2/s. In case the reader is not familiar with thermal diffusivity, it is simply the ratio of thermal conductivity to heat capacity.

Initially across the porous medium layer there is no fluid flow but there is a temperature differential from 0 °C at the flow inlet side to 100 °C at the flow outlet side. Accordingly, there is a steady-state linear temperature gradient across the layer from 0 °C to 100 °C before the fluid flow starts.

At time zero, fluid begins flowing at the specified rate and as it does so, it carries heat downstream towards the outlet side of the porous layer and thus changes the temperature profile across the layer. The boundary temperatures are maintained at 0 °C and 100 °C at the inlet and outlet sides, respectively. This causes the applied heat at the fluid outlet side to diffuse upstream against the fluid flow. Eventually a steady-state is reached whereby the temperature profile across the layer does not change with time.

The analytic solution presented in Hoffman, 2001, enables calculation of the temperature profile across the porous layer at any time after fluid flow is started, and also includes a simplified calculation of the temperature profile at thermal steady-state. The time-dependent analytic calculation is somewhat cumbersome to complete and is therefore not included here.

Figure 2 presents numerically computed temperature profiles across the porous layers at various times. The analytically computed steady-state temperature profile is also plotted for comparison. As shown in the plot, the numerically computed temperature profile at 25 seconds matches almost exactly to the numerically computed profile. It is thus evident that numerical model properly computes convective-conductive heat transport temperatures in this case.

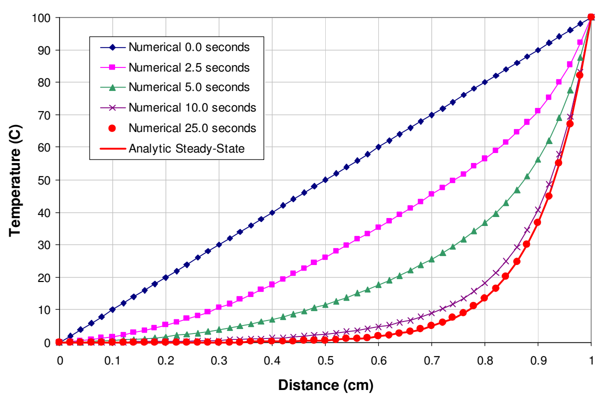

Figure 2. Comparison of Analytic and Numerical Solutions

3.2 Comparison to Expected Heat Transport Velocity

Another verification case was analyzed to compare the numerically computed heat transport distance to that expected based on the heat transport velocity as described earlier.

In this case a 1D horizontal groundwater flow field was established in a 2D modelling domain with groundwater flow from left to right. The parameters presented in Table 1 were used in this analysis. The parameters chosen for this analysis are representative of a sand/gravel aquifer and were selected to provide round numbers to facilitate comparison with the numerical solution. In particular, note that the expected heat transport velocity in this case is 0.08 m/d.

Table 1: Analysis Parameters for Heat Transport Velocity Verification Case

Parameter	Value
Hydraulic Conductivity (m/d)	5.0
Hydraulic Gradient (m/m)	0.01
Darcy Velocity* (m/d)	0.05
Porosity	0.25
Average Linear Groundwater Velocity (m/d)	0.20
Heat Capacity of Water (kJ/kg-°C)	4200
Heat Capacity of Soil Grains (kJ/kg-°C)	2100
Heat Capacity of Saturated Aquifer* (kJ/kg-°C)	2625
Ratio of Heat Capacities* (Water / Sat. Aquifer)	1.60
Expected Heat Transport Velocity* (m/d)	0.08
Modelling Domain Length (m)	160
Thermal Conductivity of Saturated Aquifer(kJ/d-m-°C)	100
Modelling Domain Half-Width (m)	80

* Derived parameter

A portion of the domain geometry and the initial conditions in the numerical model are shown in Figure 3. Initial temperatures were specified using a Gaussian distribution with a peak temperature of 100 °C centered at northing/easting coordinate (0,0) dropping to 0 °C away from the peak. Use of a smooth and physically realistic initial temperature distribution was done to avoid numerical dispersion errors which occur when an unrealistic point temperature value is specified at time zero. The temperature contours in Figure 3 range from 10 to 100 °C, therefore the white areas indicate a temperature between 0 and 10 °C.

It is important to note that the exact spread of the initial temperature distribution is not important in this analysis because the computed value of interest is the downstream movement of the thermal plume peak temperature with time.

Symmetry along the centreline of the flow field was utilized to reduce computational expense. As indicated in Table 1, the half-width of the model domain was 80 m, although in Figures 3 and 4 only part of the domain half-width is shown.

The groundwater flow is steady-state therefore the hydraulic head at all times drops linearly along the easting axis with a constant hydraulic gradient as indicated in Table 1. The groundwater flow direction is indicated in the Figures 3 and 4 by the groundwater flow path lines as indicated with arrows.

Figure 4 shows the numerically computed thermal plume after 800 days. At this time the peak temperature has reduced from 100 °C to between 50 °C and 60 °C and the radius of the 10 °C isotherm has increased from about 18 m to 21 m. Most importantly, the temperature peak has moved from an easting of 0 m to between 60 m and 65 m.

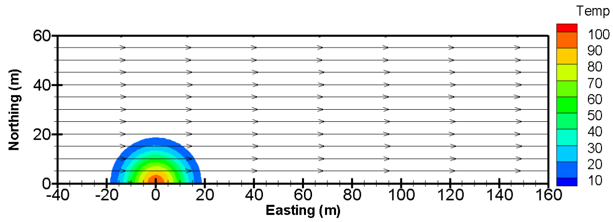

Figure 3. Initial Conditions for Heat Transport Velocity Verification Case

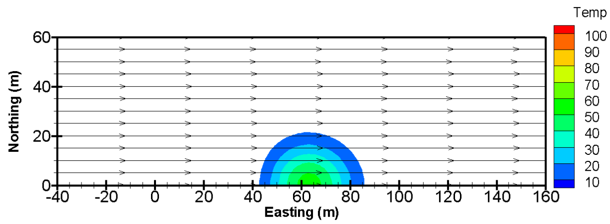

Figure 4. Temperature Distribution after 800 Days for Heat Transport Velocity Verification Case

A better view of the computed temperature data along the centreline of the flow at various times is provided in Figure 5. The figure also shows the expected location of the peak temperature based on the heat transfer velocity value presented in Table 1.

Inspection of Figure 5 shows that there is excellent agreement between the expected and numerically computed peak temperature locations. It is noted that at later times, such as 800 days, the numerically computed peak temperature downstream distance is on the order of 1 m less than the expected value. This is considered to be likely a result of numerical dispersion. It is therefore concluded that the numerical model correctly computes the expected heat transfer velocity with some small unavoidable error likely caused by numerical dispersion.

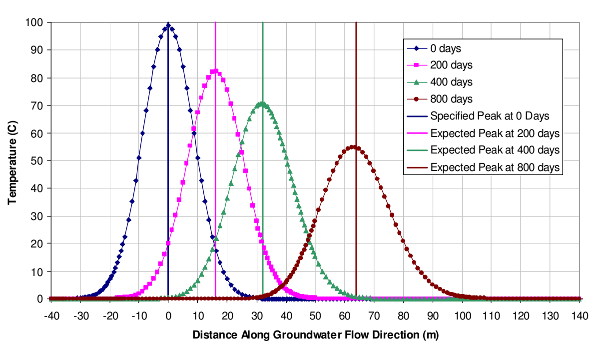

Figure 5. Comparison of Expected and Numerically Computed Heat Transport Velocities

4 TEMPERATURE DEPENDENT WATER VISCOSITY

4.1 Water Viscosity Variation with Temperature

The PDE for steady-state groundwater flow (Equation 1) includes the hydraulic conductivity of the porous medium as a material property. Hydraulic conductivity is a function of both the permeability of the porous medium and water properties as given by (Freeze and Cherry, 1979):

$$K_H = \frac{k\rho g}{\mu} \qquad [11]$$

Where:
K_H = hydraulic conductivity (m/d)
k = permeability (m^2)
ρ = density of water (kg/m^3)
g = gravitational acceleration (9.81 m/s^2)
μ = dynamic viscosity (Pa·s)

For convective heat transport calculations, a change in fluid properties as a function of temperature will have a corresponding effect on the hydraulic conductivity.

Water density does not vary appreciably as a function of temperature. For example, water density at 100 °C is 958 kg/m^3, which is only 4% less than the maximum density of 1000 kg/m^3 at 4 °C. Therefore changes to water density as a function of temperature were considered insignificant and were thus ignored in the modelling work presented later.

Water viscosity as a function of temperature is given by (Likhachev, 2003):

$$\mu = \mu_o \exp\left[\frac{E}{R(T-\theta)}\right] \qquad [12]$$

Where:
T = temperature (°C)
μ_o = 2.4055×10^{-5} Pa·s
E = 4.753 kJ/mol
R = 8.314 J/°K-mol
θ = 139.7 °K

Figure 6 shows a plot of water viscosity versus temperature from 0 °C to 200 °C. Values are shown above 100 °C because the boiling (flash) point of water increases with pressure. As shown in Figure 6, the viscosity decreases by a factor of almost 12 from 0 °C to 200 °C.

Figure 7 shows the relationship between normalized hydraulic conductivity and temperature over the same temperature range. The normalized hydraulic conductivity refers to a unit hydraulic conductivity value at a reference temperature, in this case 4 °C, which is a typical aquifer temperature in Canada. As shown in the plot, the hydraulic conductivity increases more than an order of magnitude over the temperature range shown.

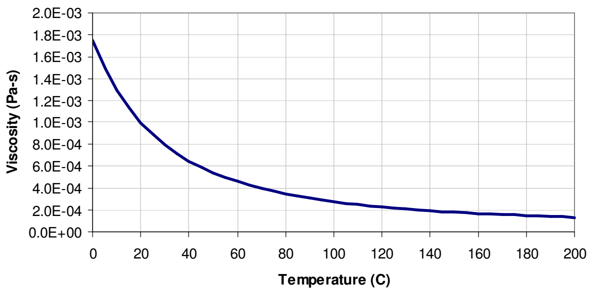

Figure 6. Water Viscosity versus Temperature

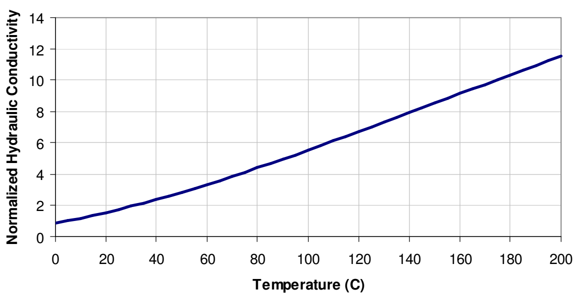

Figure 7. Normalized Hydraulic Conductivity versus Groundwater Temperature

4.2 Effect on Groundwater Flow

To help understand the effect of the coupling between the thermal and hydraulic fields caused by temperature dependent water viscosity, an analysis was performed using the all the same model parameters as described earlier for the expected heat transport velocity verification case (Figures 3 & 4). The only difference between that analysis and the one presented here was that the viscosity and thus the hydraulic conductivity was made a function of temperature.

The computed temperature distribution and groundwater flow paths after 800 days using temperature dependent water viscosity are shown in Figure 8. This figure is very informative. It is noted that the groundwater preferentially flows through the thermal plume because of its locally increased hydraulic conductivity. Furthermore, the preferential flow causes the peak temperature of the thermal plume to transport downstream at a faster rate and results in the plume taking an elliptical shape with the peak temperature located on the downstream side of the plume.

Figure 9 shows the temperature profiles along the flow centreline at various times. For comparison, this plot also shows the temperature profiles at the corresponding times for the case using a constant water viscosity. The plot shows that the preferential groundwater flow through the thermal plume causes the temperature distribution within the plume to be skewed toward its leading (downstream) edge. Interestingly, the peak temperature is not affected in this case by the preferential flow through the plume.

Based on a travel distance of the peak temperature of about 100 m in 800 days (Figure 9), the transport velocity of the temperature peak averages 0.125 m/d over this time period. This value is 2.5 times greater than the average Darcy velocity for this case of 0.05 m/d. For comparison, recall that for the case using constant water viscosity, the transport velocity of the temperature peak was 1.6 times the Darcy velocity.

It is also instructive to note that the transport velocity of the temperature peak (0.125 m/d) is in this case 0.625 times that of the average linear groundwater velocity (0.20 m/d). This indicates that groundwater inside the thermal plume moves faster than the temperature peak. The groundwater thus flows through the thermal plume, picking up heat from soil grains, transporting it downstream, and "depositing" it by warming soil grains. The groundwater thus advances the leading edge of the thermal plume faster than would occur via conductive heat transfer alone.

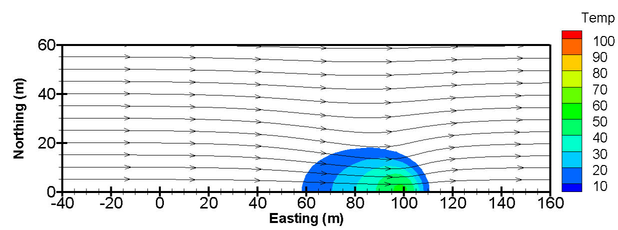

Figure 8. Temperature Distribution after 800 Days using Temperature Dependent Water Viscosity

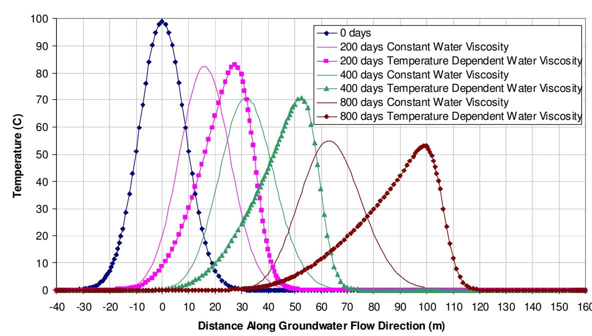

Figure 9. Temperature Profiles along Flow Centreline using Temperature Dependent Water Viscosity

5 HEAT TRANSPORT IN CONFINED AQUIFERS

Advective heat transport can be adequately modelled in 2D if the aquifer is thick relative to the length of the thermal well that penetrates it. However, where a thermal well penetrates a relatively thin aquifer confined above and below by aquitards, then vertical heat loss from the aquifer to the aquitards will attenuate transport of the thermal plume in the aquifer. In this case a 3D model is necessary.

As an illustrative example, a 20 m thick confined sand/gravel aquifer was modelled in 3D using the parameters presented in Table 2. A single thermal well at 200 °C was operated for the first 5 years of the 15 year simulation period. Note that in this case the aquifer Darcy velocity, average linear velocity and the heat transport velocity were 10, 40 and 16 m/yr, respectively.

Table 2: Analysis Parameters for Thin Confined Aquifer Case

Parameter	Value
Aquifer Hydraulic Conductivity (m/s, m/d)	$7.5x10^{-4}$, 65
Aquitard/Aquifer Hydraulic Conductivity Contrast	10^{-4}
Horizontal Hydraulic Gradient – Constant (m/m)	0.00042
Darcy Velocity * (m/d, m/yr)	$27x10^{-3}$, 10
Porosity	0.25
Average Linear Groundwater Velocity* (m/d, m/yr)	$110x10^{-3}$, 40
Heat Capacity of Water (kJ/m3-°C)	4200
Heat Capacity of Soil Grains (kJ/m3-°C)	2100
Heat Capacity of Sat. Porous Medium* (kJ/m3-°C)	2625
Ratio of Heat Capacities* (Water / Sat. Aquifer)	1.60
Heat Transport Velocity* (m/d, m/yr)	$44x10^{-3}$, 16
Thermal Conductivity (kJ/d-m-°C, W/m-°C)	250, 2.9
Aquifer Half-Thickness (m)	10
Aquitard Thickness (m)	50
Depth to Aquifer – Nominal (m)	170
Pressure in Aquifer – Nominal (kPa)	1660
Water Flash Temp. at Aquifer Depth – Nominal (°C)	200
Insitu Temperature at Aquifer Depth – Nominal (°C)	4
Thermal Well Temperature (°C)	200
Thermal Well Operating Time (years)	0 to 5
Total Simulation Time (years)	15

* Derived parameter.

Unless otherwise stated in the above, material properties are same for both the aquifer and the vertically adjacent aquitards.

The thermal plume at 5, 7, 11 and 15 years is presented in Figures 10 to 13. Specifically the plots show the location of the 10, 20 and 50 °C isotherm surfaces.

For orientation, the thermal well is located along the z-axis (at x=0, y=0). Note that to reduce computational expense, symmetry was utilized in the analysis. A horizontal symmetry plane exists at the mid-elevation of the aquifer and a vertical symmetry plane exists parallel to the groundwater flow path intersecting the thermal well. Therefore the modelling domain consists of a 10 m half-thickness horizontal aquifer overlain by 50 m thick aquitard layer.

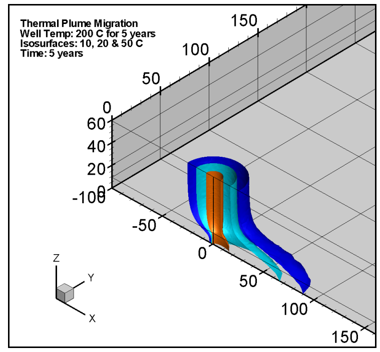

Figure 10. Thermal Plume at 5 Years

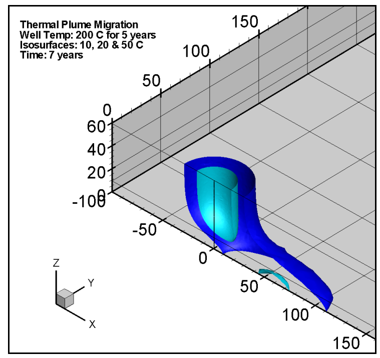

Figure 11. Thermal Plume at 7 Years

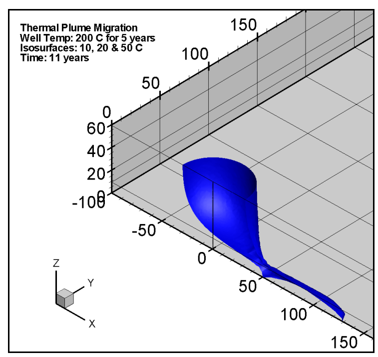

Figure 12. Thermal Plume at 11 Years

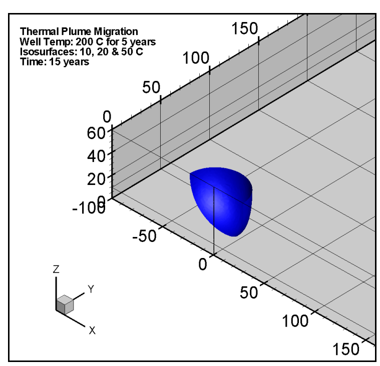

Figure 13. Thermal Plume at 5 Years

Steady-state groundwater flow parallels the x-axis which is established by a constant hydraulic gradient applied across the x-minimum and x-maximum planes of the model. There is therefore no component of groundwater flow in the y- or z-directions. The aquitard hydraulic conductivity is 4 orders of magnitude lower than that of the aquifer.

Figure 10 shows the thermal plume after 5 years corresponding to the end of thermal well operations. In the aquitard the low groundwater flow velocity results in diffusion dominated heat transport as evidenced by the near circular shape of the isotherms in the x-y plane. In contrast, the isotherms in the aquifer have an elliptical shape consistent with advection dominated heat transport.

Heat flow is perpendicular to the isotherm surfaces. Figure 10 shows that heat is transferred vertically from the aquifer to the aquitard downstream of the thermal well. In contrast, heat flows from the aquitard to the aquifer just upstream of the thermal well.

It is worth noting that the hand-calculated heat transfer velocity in this case is 16 m/year and that after 5 years the first heat from the thermal well would be expected to have travelled roughly 80 m downstream. Figure 10 shows that after 5 years the 10 °C isotherm is nominally 90 m downstream. In this situation the influence of both temperature dependent water viscosity and vertical heat loss have opposite effects on the heat transport velocity. It is therefore reasonable that the 10 °C isotherm location and the heat transport distance based on the basic heat transport velocity are similar.

After operation of the thermal well ceases at 5 years, the thermal plume continues moving downstream and the maximum plume temperature declines as heat is dissipated. At the end of 7 years the peak temperature has dropped below 50 °C but remains above 20 °C as shown in Figure 11. In fact, Figure 11 shows that the thermal plume is dividing into two separate warm water zones, one associated with the aquifer and the other associated with the aquitard. At 11 years (Figure 12) the 10 °C isotherm surfaces of these two zones have nearly separated completely. After 15 years (Figure 13) the peak temperature in the aquifer has dropped below 10 °C while in the aquitard the maximum temperature remains between 10 and 20 °C.

This example illustrates how a thermal plume evolves through time in a relatively thin aquifer. It is noteworthy that even a simplified analysis such as this, using homogeneous and isotropic material properties in a basic aquifer/aquitard system with steady-state groundwater flow, transport of the thermal plume can only be calculated using a 3D numerical model.

6 CONCLUSIONS

Based on the work presented herein, it is concluded that heat transport velocity can be quickly hand-calculated based on the ratio of water heat capacity to the porous medium capacity multiplied by the Darcy velocity. This heat transport velocity does not account for effects of temperature dependent water viscosity and only considers the velocity along a single dimension or conceptually along a flow stream tube.

In practice, the heat transport velocity in an aquifer can be reasonably estimated as 1.6 times the Darcy velocity in the absence of better information.

The governing equations presented were used to numerically compute advective heat transfer in steady-state groundwater flow. The numerical calculations were verified by comparison with an analytic solution and by comparison with the expected thermal plume transport distance based on the hand-calculated heat transport velocity.

It is necessary to include the effect of temperature dependent water viscosity in advective heat transport models especially in cases with high temperatures at the heat source. In these cases the thermal plume becomes a preferential groundwater flow zone and increases its transport velocity above the expected heat transport velocity.

Finally, in some cases it is necessary to model heat transport cases in 3D. In the case of a thin confined aquifer, 3D analysis is required to account for vertical heat transfer into the confining aquitards.

ACKNOWLEDGEMENTS

The author thanks the reviewers of this paper for their time and helpful comments.

REFERENCES

Andersland, O.B. and Ladanyi, B., 2004. *Frozen Ground Engineering, Second Edition*, John Wiley & Sons Inc., Hoboken, N.J., USA

Freeze, R.A. and Cherry, J.A., 1979. *Groundwater*, Prentice-Hall Inc., Englewood Cliffs, N.J., USA

Hoffman, J.D., 2001. *Numerical Methods for Engineers and Scientists*, McGraw-Hill Inc., New York, NY, USA

Likhachev, E.R., 2003. Dependence of Water Viscosity on Temperature and Pressure, *Technical Physics*, 48(4): 514-515

Neild, D.A. and Bejan, A., 2006. *Convection in Porous Media, Third Edition*, Springer Publishers. New York, NY, USA